Toxicology in Vitro 90 (2023) 105611

Contents lists available at ScienceDirect

Toxicology in Vitro

journal homepage: www.elsevier.com/locate/toxinvit

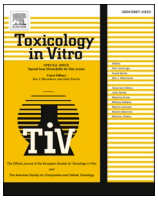

Characterization of elements, PAHs, AhR-activity and pro-inflammatory responses of road tunnel-derived particulate matter in human hepatocyte-like and bronchial epithelial cells

Jørn A. Holme [a], Marit Låg [a,*], Tonje Skuland [a], Martina Parenicová [b], Miroslav Ciganek [b], Katerina Penciková [b], Vegard Sæter Grytting [a], Jiri Neca [b], Johan Øvrevik [c,d], Espen Mariussen [a], Rikke Bramming Jørgensen [e], Magne Refsnes [a], Miroslav Machala [b]

[a] Department of Air quality and Noise, Division of Climate and Environmental Health, Norwegian Institute of Public Health, PO Box 222 Skøyen, 0213 Oslo, Norway
[b] Department of Pharmacology and Toxicology, Veterinary Research Institute, 62100 Brno, Czech Republic
[c] Department of Biosciences, Faculty of Mathematics and Natural Sciences, University of Oslo, PO Box 1066 Blindern, 0316 Oslo, Norway
[d] Division of Climate and Environmental Health, Norwegian Institute of Public Health, PO Box 222 Skøyen, 0213 Oslo, Norway
[e] Department of Industrial Economics and Technology Management, Norwegian University of Science and Technology, NTNU, Trondheim, Norway

ARTICLE INFO

Editor: Dr. Martin Leonard

Keywords:
Air pollution
Diesel exhaust particles
Inflammation
Metals
Polyaromatic compounds
Aryl hydrocarbon receptor (AhR)
Airway epithelial cells

ABSTRACT

The aims were to characterize the content of elements and polycyclic aromatic hydrocarbons (PAHs) in size-separated particulate matter (PM) sampled in a road tunnel, estimate the contribution of PAHs to the toxic potential, and measure the pro-inflammatory potential of PM samples and extracts with increasing polarity. Several elements/metals previously associated with cytokine responses were found. Based on PAHs levels and published PAHs potency, the calculated mutagenic and carcinogenic activities of size-separated samples were somewhat lower for coarse than fine and ultrafine PM. The AhR-activity of the corresponding PM extracts measured in an AhR-luciferase reporter model (human hepatocytes) were more similar. The highest AhR-activity was found in the neutral (parent and alkylated PAHs) and polar (oxy-PAHs) fractions, while the semi-polar fractions (mono-nitrated-PAHs) had only weak activity. The neutral and polar aromatic fractions from coarse and fine PM were also found to induce higher pro-inflammatory responses and CYP1A1 expression in human bronchial epithelial cells (HBEC3-KT) than the semi-polar fractions. Fine PM induced higher pro-inflammatory responses than coarse PM. AhR-inhibition reduced cytokine responses induced by parent PM and extracts of both size fractions. Contributors to the toxic potentials include PAHs and oxy-PAHs, but substantial contributions from other organic compounds and/or metals are likely.

1. Introduction

Epidemiological studies have observed strong associations between exposure to ambient particulate matter (PM) and respiratory effects, including development and/or exacerbation of asthma and chronic obstructive pulmonary disease (COPD) (Dominski et al., 2021), increased occurrence of respiratory infections (Ziou et al., 2022) and lung cancer (Pyo et al., 2022), as well as increased mortality (Stafoggia et al., 2022). Many of the PM-associated adverse health effects are known to involve inflammatory processes (Borm et al., 2022). However, it remains unclear what chemical components or physical characteristics of PM are responsible for the observed adverse effects (Låg et al., 2020; Øvrevik et al., 2017; Øvrevik et al., 2015).

The oxidative potential of PM has been suggested to be an important

Abbreviations: Aryl hydrocarbon receptor, AhR; benzo[*a*]pyrene, B[*a*]P; chemokine CXC-motif ligand 8, CXCL8; chronic obstructive pulmonary disease, COPD; cytochrome P450 1A1, CYP1A1; dioxin response elements, DREs; diesel exhaust particles, DEP; dithiothreitol, DTT; neutral aromatic fractions, parent and alkylated PAHs, E1; semi-polar aromatic fraction, mononitrated-PAHs, E2; polar aromatic fractions, oxy-PAHs, E3; elemental carbon, EC; human bronchial epithelial cells, HBEC3-KT; interleukin, IL; lactate dehydrogenase, LDH; *N*-acetyl salicylic acid, NAC; organic carbon, OC; particulate matter, PM; polycyclic aromatic hydrocarbons, PAHs; PM-extractable organic material, EOM; reactive oxygen species, ROS; residual particles after the extractions, PM-EOM; standard error of mean, SEM; 2,3,7,8-tetrachlorodibenzo-p-dioxin, TCDD.

* Corresponding author.
E-mail address: marit.lag@fhi.no (M. Låg).

https://doi.org/10.1016/j.tiv.2023.105611
Received 1 February 2023; Received in revised form 26 April 2023; Accepted 3 May 2023
Available online 8 May 2023

parameter associated with inflammation and toxicity following ambient PM exposure (Campbell et al., 2019), and metals associated to the particles have been suggested as potential environmental stressors for chronic diseases (Schiavo et al., 2022). Elements/metals such as iron, vanadium, and copper may contribute to acellular oxidative PM potential, participating in the generation of reactive oxygen species (ROS) by redox-mediated mechanisms. PM and associated elements may additionally induce cellular ROS formation. ROS as well as some metal ions may inactivate proteins and enzymes by reacting with thiol groups and seem to be involved in toxicity as well as inflammatory responses. Following exposure, PM and its adsorbed metal components may stimulate the release of pro-inflammatory cytokines (Låg et al., 2016; Låg et al., 2010; Øvrevik et al., 2017). Metals or metalloids associated with health effects of ambient PM include zinc (Zn^{2+}), arsenic (As^{3+}), nickel (Ni^{2+}), iron (Fe^{2+}), copper (Cu^{2+}), vanadium (VO_4^{3-}) and manganese (Mn^{2+}) (Chen and Lippmann, 2009).

The content of organic carbon (OC) may also be an important contributor to both respiratory disease and mortality (Cassee et al., 2013). Traffic-PM contains organic species, including alkanes, alkenes, aromatics, oxygenated compounds (such as aldehydes, ketones and carboxylic acids), amino compounds, nitrates, and polycyclic aromatic hydrocarbons (PAHs) (Seinfeld and Pandis, 1998). PAHs and PAH-derivatives are considered an important part of the OC attached to the particle core, with documented biologic activity and toxic potential (Kermani et al., 2021; Låg et al., 2020; WHO, 2000; Øvrevik et al., 2015). While high-molecular weight PAHs containing five or more aromatic rings are mainly found bound to PM, the smaller PAHs containing four or fewer aromatic rings are found to a greater extent in the gas phase, although their relative distribution is highly dependent on temperature (Srogi, 2007). Accordingly, PAHs levels attached to PM during winter may be up to ten-fold higher compared to summer (Gualtieri et al., 2010).

Road traffic is considered an important source of PM-associated PAHs, as well as the more hydrophilic and mobile polar PAHs-derivatives including nitrated PAHs (nitro-PAHs) and oxygenated PAHs (oxy-PAHs) (Keyte et al., 2016). In addition to direct formation from combustion of diesel and gasoline, the oxy- and nitro-PAHs may be formed via reactions of primary PAH with atmospheric oxidants. However, compounds like 1-nitropyrene and 3-nitrofluoranthene are mainly derived directly from diesel engine emissions (Anders Feilberg and TorbenNielsen, 2001). Based partly on occurrence and partly on toxicity, special attention has been given to the 16 PAHs classified as priority pollutants (USEPA, 2005). These do not include oxy-PAHs and nitro-PAHs (Andersson and Achten, 2015). The occurrence and knowledge regarding the potential toxicity of these substituted compounds compared to unsubstituted PAHs are limited (Machala et al., 2001a). However, studies report that some oxy- and nitro-PAHs exert effects linked to cytotoxicity, immunotoxicity, mutagenicity and carcinogenicity in experimental systems (Durant et al., 1996; IARC, 2013; IARC, 2014; WHO, 2000). Similarly, many non-priority PAHs with reported toxic potencies (Machala et al., 2001b; Vondráček et al., 2017) should be included into the future risk assessment and understanding of PM toxicity.

The biological responses initiated by PAH and PAHs-derivatives include binding to and activation of receptors such as the aryl hydrocarbon receptor (AhR) (Låg et al., 2020; Vondrácek et al., 2011; Øvrevik et al., 2017). AhR-mediated metabolism of PAHs can also contribute to the generation of ROS, oxidative stress and oxidative DNA damage. In addition, parent compounds and reactive PAH-metabolites may directly interfere with essential molecular sites on macromolecules, including DNA, ion transporters and enzymes involved in signal transduction, such as mitogen-activated protein kinases and Akt kinase, with implications for disease development (Låg et al., 2020; Vondráček and Machala, 2021). AhR activation is also involved in modulation of inflammatory signals (Ishihara et al., 2019; Vondrácek et al., 2011).

Road tunnels provide a useful environment for sampling traffic-related PM for chemical and biological characterization due to stable temperatures and little input from other primary sources. Very few studies have extensively characterized the chemical composition of road tunnel PM in combination with assessment of biological effects (Keyte et al., 2016; Skuland et al., 2022). Recently, we sampled coarse, fine and ultrafine PM in two road tunnels under humid and dry road surface conditions and characterized them with regard to hydrodynamic size distribution, content of elemental carbon (EC), organic carbon (OC), endotoxin, and the capacity for acellular generation of ROS and induction of cytokine release (pro-inflammatory potentials) in human bronchial epithelial cells (HBEC3-KT) (Skuland et al., 2022). Linear correlation analysis showed that particle-induced cytokine responses were correlated to OC levels, while no correlations were observed for the other PM characteristics. A follow-up study of selected road tunnel PM samples supported a potential causal role for the OC, as the pro-inflammatory responses were reduced by a chemical inhibitor of AhR (CH223191) and co-treatment with the antioxidant *N*-acetylcysteine (Refsnes et al. submitted 2023).

The aims of the current study were to characterize coarse, fine and ultrafine PM samples from one of the road tunnels more completely with regard to: i) the content of elements, PAHs, oxy-PAHs and nitro-PAHs and to estimate the PAHs' mutagenic/carcinogenic/AhR-activating potencies and ii) to elucidate any potential role of elements and PAHs/PAH-derivatives in the PM-induced cellular effects, including AhR-activity and pro-inflammatory responses.

2. Methods

2.1. Materials

HBEC3-KT cells (passage 4–35; (ATCC CRL-4051) were bought from ATTC (Manassas, Virginia, US). The cell culture flasks were purchased from Nunc A/S, Roskilde, Denmark, while the cell culture plates were from Corning, NY 14831 USA. PureCol collagen was from Advanced BioMatrix, Inc., CA, USA. The cell culture media LHC-9 and DMEM:F12, and Trypsin-EDTA were obtained from Gibco, Thermo Fisher Scientific, Waltham, MA, USA. The Cytotoxicity Detection Kit using lactate dehydrogenase (LDH) activity was bought from Merck KGaA, Darmstadt, Germany. The sandwich enzyme-linked immunosorbent assay (ELISA) cytoset for determination of chemokine CXCL8 was purchased from Invitrogen, Thermo Fisher Scientific, Waltham, MA, USA, while the IL-1α DuoSet was from R&D Systems, Inc., Minneapolis, MN, USA. Whatman TE 38 filter was from (Whatman, Maidstone, Kent, UK). The RNA isolating kit; NucleoSpin RNA plus, was obtained from MACHEREY-NAGEL, Duren, Germany. High Capacity cDNA Archive Kit, TaqMan Universal PCR Mastermix and TaqMan Gene Expression Assays for IL1A, CXCL8, HMOX1, CYP1A1, PTGS2/COX2 and GAPDH were bought from Applied Biosystems. CH223191 was bought from Merck KGaA, Darmstadt, Germany. PAHs, oxy-PAHs and nitro-PAHs for analytical confirmation were obtained from Promochem (Wesel, Germany). Other chemicals were purchased from commercial sources at the highest purity available.

2.2. PM samples

Traffic-derived coarse PM (10–2.5 μm), fine PM (2.5–0.18 μm) and ultrafine PM (quasi-ultrafine; < 0.18 μm) were sampled inside a road tunnel during dry surface conditions in late winter season (March 2019; Hell tunnel, Trondheim, Norway). The average tunnel temperature was 14.9 °C and average relative humidity 60.5%. The tunnel has a speed limit of 80 km/h, with approximately 16,000 vehicles passing through per 24 h. Approximately 40% of the vehicles used studded tires and 17% were heavy duty vehicles. PM of different sizes were sampled by a high-volume cascade impactor 10 days after a comprehensive washing of the tunnel at a flow rate of 900 L/h in 10–12 h periods. The sampler had a multistage round slit nozzle, and polyurethane foam (PUF) was used as

impaction substrate for the coarse and fine PM, and a Whatman TE 38 filter for the ultrafine PM. The collected PM samples were extracted from the PUFs and filters by methanol combined with vortex/sonication to dislodge the particles from the filters, whereafter methanol was removed by a rotary evaporator. The PM samples were suspended in pyrogen-free sterile water (10 mg/mL), vortexed, sonicated and stored at −20 °C. Before use the PM were vortexed and sonicated once more. The hydrodynamic size distribution, concentrations of organic (OC) and elementary carbon (EC), endotoxin content of the PM samples, and their ability to generate acellular ROS have been published elsewhere (Skuland et al., 2022) and are summarized in Table 1. The large hydrodynamic size of the ultrafine PM measured (peak 2.2 μm based on mass) is due to an unavoidable secondary aggregation/agglomeration as a result of sampling, but a contamination of fine PM cannot be excluded.

2.3. Element analysis of size-separated PM

The size-separated tunnel particles and the water phase in which the particles were dissolved, were analysed for a range of elements by inductively coupled plasma mass spectrometry (ICP-MS). The analyses were performed by Norwegian Institute of Air Research (NILU) which is accredited by the Norwegian Accreditation (NS-EN ISO/IEC 17025) as an analysis laboratory for metals in various matrices, such as geological materials and water. In brief, aliquots of the particles resuspended in water were transferred on pre-weighed filters (55 mm Munktel filter paper) by vacuum filtration. The filters were dried in room temperature, split in two and weighed. Each half of the filters were then transferred to Teflon containers and subjected to micro-wave-assisted digestion in an UltraCLAVE single reaction chamber microwave oven (Milestone, Italy) by HNO_3 and HF + HNO_3, respectively. The digests and the filtrates were then diluted in ultrapure deionized MQ-water (water purified using a Millipore Milli-Q lab water system), and elements were analysed by ICP-MS (Agilent 7700× Agilent, Santa Clara, CA, USA), using the method accredited according to requirements of NS-EN/IEC 17025 (NILU-U-110, NILU-U-112).

2.4. Extraction, fractionation and chemical analysis of size-separated PM

Chemicals from the road-tunnel PM samples were extracted and fractionated based on different polarity as previously described for standardized reference diesel exhaust PM (Andrysík et al., 2011; Pálková et al., 2015). In short, samples of coarse, fine and ultrafine PM were evaporated to dryness. The residues were re-dissolved in hexane and applied to the top of the open Silica gel 60 column, activated for 1 h at 200 °C (particle size 0.063–0.2 mm; Merck, Darmstadt, Germany). The column with dimensions 250 × 10 mm was dry-packed with 10 g of activated silica gel and washed with 30 mL of hexane prior to application of sample. Fractionation of extracts (E) was done by gradual elution with 20 mL of hexane to obtain E0 (an aliphatic fraction not further analysed here), followed by 27 mL of hexane/dichloromethane (1:1, *v*/v) resulting in E1 (neutral fraction with parent and alkylated PAHs), 20 mL of dichloromethane ending up in E2 fraction (semi-polar compounds including mono- and di-nitrated derivatives of PAHs) and, finally, by 30 mL of methanol (E3, polar fraction, which contained polar compounds, including oxygenated derivatives of PAHs). The recovery of extraction/fractionation steps was 70–90%. The concentrations of PAHs in the crude extract (CE) and E1 fraction are comparable, as previously confirmed by an independent analysis of both matrices (Andrysík et al., 2011). The methodology of extraction and fractionation used are noninvasive techniques. The high-performance liquid chromatography (HPLC) equipped with a photodiode array detector (DAD), liquid chromatography/ mass spectrometry (LC/MS)–MS system with triple quadrupole mass spectrometer and electrospray ionisation (ESI) or atmospheric pressure chemical ionisation (APCI) ion sources and a gas chromatography (GC) system coupled with ion trap mass spectrometer were used for identification and quantification of aromatic compounds in E1, E2 and E3 fractions of coarse, fine and ultrafine PM. Further details on chemical analysis are described elsewhere (Andrysík et al., 2011). Another part of E1, E2 and E3 was evaporated and dissolved in DMSO, and the residual particles after the extractions (PM-EOM) were centrifuged and resuspended in DMSO and stored at −20 °C for biological studies.

Table 1
Characterization of road tunnel PM.

Characteristics	Coarse PM	Fine PM	Ultrafine PM
Hydrodynamic size (by mass, μm)	3.01	1.56	2.22/0.07
Hydrodynamic size (by number, μm)	0.05	0.06	0.07
Organic carbon (OC, mg/mg PM)	28 ± 10	94 ± 37	131 ± 29
Elementary carbon (EC, mg/mg PM)	0	0	0
Endotoxin content (EU/mg PM)	0.61 ± 0.29	0.25 ± 0.13	0.09 ± 0.09
ROS (OP^{DDT}; nmol DTT/ng*min))	0.038	0.043	0.013

2.5. AhR-activity of chromatographic fractions in human AZ-AhR cells

AhR-mediated ("dioxin-like") activities of the polarity-based E1, E2 and E3 fractions of the PM samples were determined in the AZ-AhR reporter cell line, a human hepatocellular carcinoma cells (HepG2) stably transfected with several dioxin response elements (DREs) upstream of a luciferase reporter gene (Novotna et al., 2011). Cells were incubated for 24 h with the test compounds and/or vehicle (DMSO; 0.1% *v*/v), in the presence or absence of 2,3,7,8-tetrachlorodibenzo-p-dioxin (TCDD) (5 nM; AZ-AhR cells). After the treatment, cells were lysed and luciferase activity was determined using Luciferase Assay Kit (BioThema, Handen, Sweden). AhR-mediated activities of individual PAHs were calculated from presented concentration data and previously reported induction equivalency factors of individual PAHs (Vondráček et al., 2017) and expressed as pg TCDD/mg PM.

2.6. AhR-activity of chromatographic fractions in rat hepatoma H4IIE cells

AhR-mediated activities of individual PAHs were also calculated from presented chemical data and previously reported induction equivalency factors of individual PAHs developed in DR-CALUX assay (BDS, Amsterdam, The Netherlands) in rat hepatoma H4IIE cells stably transfected with a luciferase reporter gene under the control of dioxin-responsive enhancers (Machala et al., 2001b; Vondrácek et al., 2001).

2.7. Culturing and exposure of HBEC3-KT cells

HBEC3-KT cells were cultured in LHC-9 medium in collagen-coated flasks (PureCol) and maintained in a humified atmosphere at 37 °C containing 5% CO_2 as previously described (Låg et al., 2018). Three days before exposure to PM/PM-extracts and/or vehicle (DMSO; 0.2% v/v), the cells were seeded on pre-coated 6-well plates at a density of 170.000 cells/cm^2. Serum-free DMEM:F12 (1:1) was used one day before and during exposure. Cells and cell culture media were collected after 20 h exposure, centrifuged and stored at −80 °C until further analyses.

2.8. Cytotoxicity

PM-induced cytotoxicity in HBEC3-KT cells was examined by the lactate dehydrogenase (LDH) assay. The cellular release of LDH into the media was measured according to the manufacturer's guidelines (Roche, Germany) using TECAN Sunrise plate reader (Männedorf, Switzerland).

2.9. Cytokine analysis

The concentrations of IL-1α and CXCL8 released from HBEC3-KT cells into the cell culture media following exposure of PM/PM-extracts

were determined by ELISA according to the manufacturer's guidelines, using a TECAN Sunrise plate reader (Männedorf, Switzerland) equipped with a dedicated software (Magellan V 1.10).

2.10. Gene expression analysis

RNA was isolated from HBEC3-KT cells using the RNA isolation kit NukleoSpin RNA plus according to the supplier's recommendations. Gene expression of IL1A (Hs00174092_m1), CXCL8 (Hs00174103_m1), CYP1A1 Hs00153120_m1), PTGS2/COX2 (Hs00153133_m1), and HMOX1/HO-1 (Hs01110250_m1)) was analysed by qPCR using BioRads CFX96 Touch Real-Time PCR Detection System, with pre-designed TaqMan Gene Expression Assays and TaqMan Universal PCR Master Mix. Total RNA (0.5–1 μg) was reverse transcribed to cDNA in 25 μL (using a High-Capacity cDNA Archive Kit). cDNAs were next diluted 1:100 in a solution of nuclease-free water, TaqMan Universal master mix and TaqMan Gene Expression before performing the qPCR. The expression of each gene was normalized against house-keeping genes (GAPDH) and expressed as mean ± SEM (fold) compared to the untreated control by the ΔΔCt-method.

2.11. Statistical analysis

Statistical analyses of 3–4 independent biological replicates with HBEC3-KT cells were performed by using two-way ANOVA with Dunnett's Multiple comparison test (using GraphPad Prism software (version 8.0 Inc., San Diego, CA).

3. Results

3.1. PM characterizations

3.1.1. Metals

As presented in Table 2, we analysed the content of 24 elements analysed by ICP-MS, which represented 17, 18 and 19% of the total mass in coarse, fine and ultrafine PM, respectively. The relative pattern of crustal elements (Mg, Al, Si, Ca and Fe) was rather similar between the size-separated PM samples and represented a large proportion of total element mass of all samples (98%). However, higher levels of Cu, Mo, Sn, Sb and Ba were observed in the fine PM than coarse and ultrafine PM.

Table 2
Concentrations of elements/metals in road tunnel PM.

Elements	Coarse PM	Fine PM	Ultrafine PM
Be	0.52	0.32	0.35
Mg	9535	8084	7270
Al	21,979	17,101	16,295
Si	95,673	108,843	127,114
Ca	19,046	12,932	14,274
Ti	1660	1886	1848
V	61.3	68.6	71.8
Cr	53.5	81.5	43.3
Mn	412	397	314
Fe	24,365	26,847	18,624
Co	16.3	17.2	12.0
Cu	130	378	107
Zn	381	412	279
As	2.63	2.71	2.08
Sr	113.4	79.3	83.3
Mo	3.47	15.59	3.83
Cd	0.09	0.09	0.23
Sn	20.7	92.4	22.3
Sb	22.6	97.8	25.7
Cs	1.18	1.04	0.91
Ba	184	329	211
W	57.3	83.0	51.6
Pb	7.98	8.20	7.03
U	0.95	0.77	0.76

The elements in the different size-separated PM as ng/mg PM.

Notably, Zn a metal with known inflammatory potential, was detected in all PM size fractions. In addition, the redox-active Fe and Cu, together with substantial amounts of V were detected. Other metals associated with health effects of ambient air detected on the road tunnel PM include Mn and Pb.

3.1.2. PAHs and PAHs derivatives

The content of US EPA priority PAHs, other PAHs, oxy-PAH, and nitro-PAHs in the size-separated road tunnel PM samples is presented in Table 3. Parent and alkylated PAHs were exclusively found in the E1 neutral aromatic fraction (Ciganek et al., 2004; Pálková et al., 2015), and their levels are presented in Table 3. More US EPA PAHs were found in the ultrafine and fine PM samples than in coarse PM, with phenanthrene>pyrene>fluoranthrene being the most abundant species (Table 3A). Overall, lower concentrations of the carcinogenic PAHs were found in the coarse PM sample. However, coarse PM had higher accumulation of high-molecular-weight (MW) PAHs like benzo[*ghi*]perylene, indeno[1,2,3-*cd*]pyrene and coronene. Higher accumulation of PAHs with MW 228 (benz[*a*]anthracene, chrysene; 4 rings), 252 and 278 (benzo[*a*]pyrene, benzo[*e*]pyrene, benzo[*k*]fluoranthene, benzo[*j*]fluoranthene, dibenz[*a,h*]anthracene; 5 rings) was detected in the fine PM samples. Importantly, high concentrations of the strong mutagen

Table 3
Concentrations of PAHs in road tunnel PM.

A. The concentrations of US EPA PAHs in coarse ($PM_{10–2.5}$), fine ($PM_{2.5–0.18}$) and ultrafine ($PM_{0.18}$). PM (ng/mg PM) sampled in a road tunnel and analysed by HPLC. *; carcinogenic PAHs

US EPA PAHs	Coarse PM	Fine PM	Ultrafine PM
Fluorene	<0.05	0.23	0.28
Phenanthrene	3.4	7.4	9.1
Anthracene	0.05	0.33	0.37
Fluoranthene	1.3	3.8	4.9
Pyrene	1.7	4.9	7.0
Benz[*a*]anthracene (*)	0.08	0.52	0.29
Chrysene (*)	0.07	0.78	0.45
Benzo[*b*]fluoranthene (*)	0.05	0.09	0.17
Benzo[*k*]fluoranthene (*)	0.09	0.15	0.11
Benzo[*a*]pyrene (*)	0.38	0.62	0.45
Dibenz[*a,h*]anthracene (*)	0.04	0.04	0.03
Benzo[*ghi*]perylene	0.84	0.29	0.18
Indeno[1,2,3-*cd*]pyrene (*)	0.34	0.27	0.19
Sum of US-EPA PAHs	*8.3*	*19.5*	*23.5*
Total carcinogenic PAHs (*)	*1.0*	*2.5*	*1.7*
% of carcinogenic PAHs (*)	*12.6*	*12.7*	*7.1*

B. The concentrations of some PAHs beyond US EPAs' in coarse ($PM_{10–2.5}$), fine ($PM_{2.5–0.18}$) and ultrafine ($PM_{0.18}$). PM (ng/mg PM) sampled in a road tunnel and analysed by HPLC. Limit of quantification (LOQ) = 0.01 ng/mg PM

Other PAHs	Coarse PM	Fine PM	Ultrafine PM
Biphenyl	<0.01	<0.01	<0.01
4H-Cyclopenta[*def*]phenathrene	<0.01	0.34	0.37
Benzo[*ghi*]fluoranthene	<0.01	<0.01	<0.01
Benzo[*c*]phenanthrene	<0.01	0.15	0.06
Cyclopenta[*cd*]pyrene	<0.01	0.57	0.67
Triphenylene	<0.01	<0.01	<0.01
Benzo[*a*]fluoranthene	0.07	0.16	0.16
Benzo[*j*]fluoranthene	0.28	0.32	0.25
Benzo[*e*]pyrene	0.26	0.37	0.23
Perylene	0.11	0.14	<0.01
Dibenz[*a,c*]anthracene	<0.01	<0.01	<0.01
Dibenz[*a,j*]anthracene	<0.01	<0.01	<0.01
Picene	<0.01	<0.01	<0.01
Coronene	1.05	0.27	0.15
Benzo[*b*]chrysene	<0.01	<0.01	<0.01
Benzo[*c*]chrysene	<0.01	<0.01	<0.01
Sum of other PAHs	*1.8*	*2.3*	*1.9*

Parent and alkylated PAHs are exclusively found in the E1 neutral aromatic fraction (Ciganek et al., 2004; Pálková et al., 2015).

cyclopenta[*cd*]pyrene were found in the fine and ultrafine PM samples. On the other hand, 6-ring PAHs, such as the highly mutagenic dibenzo [*a,l*]pyrene, were not detected in the samples (Table 3B).

Previous studies have shown that the oxy-PAHs, dinitro-pyrenes and nitro-oxy-PAHs, such as 3–3-nitrobenzanthrone, as well as several other polar aromatic compounds (mostly unidentified) are extracted in the polar E3 fraction (Ciganek et al., 2004; Pálková et al., 2015). When analysing this fraction from the coarse, fine and ultrafine road tunnel samples, the highest concentrations of oxy-PAHs were detected in the ultrafine PM, followed by the fine PM (Table 4A). Anthrone was found to be the dominating oxy-PAH, followed by 9H-fluoren-9-one. Dinitrated PAHs (dinitropyrene) were not detected (Supplementary Table 1S).

E2 fractions have been reported to contain semi-polar compounds and include all mono-nitro-PAHs extracted from PM (Ciganek et al., 2004; Pálková et al., 2015). As shown in Table 4B, mono-nitro-PAHs accumulated mainly in the fine and ultrafine PM samples, with the highest content of 1-nitronaphthalene and 9-nitroanthracene. In addition, the concentration of 1-nitropyrene was much higher in the ultrafine and fine PM samples compared with the coarse PM.

3.1.3. Calculated mutagenic and carcinogenic potencies

DNA damage and mutation are considered central modes of actions for carcinogenic PAHs, in addition to other effects, including AhR-activity linked to increased cell proliferation and inflammation, that are known to potentiate the effects of genotoxic PAHs (Boström et al., 2002). Thus, information regarding the levels of PAHs in size-separated PM samples may contribute to an increased understanding of potential health risk of urban air.

Mutagenic potencies as calculated from mutagenic equivalency factors (Durant et al., 1996; Durant et al., 1999) and concentrations of individual PAHs on PM mass (ng/mg) are presented in Table 5. The calculated overall mutagenicity of fine and ultrafine PM was 7 to 8 times higher than that from coarse PM. Cyclopenta[*cd*]pyrene was the most prominent contributor to the estimated mutagenicity of the individual PAHs found in the fine and ultrafine PM, followed by benzo[*a*]pyrene (B[*a*]P). While the calculated mutagenicity of B[*a*]P was in the same order in the three size-separated PM samples, cyclopenta[*cd*]pyrene was not detected in the coarse sample. The concentration of the most potent mutagenic PAH (dibenzo[*a,l*]pyrene) was under the limit of detection.

Carcinogenic potencies presented in Table 6 were calculated from carcinogenic equivalency factors of individual PAHs estimated relativly to B[*a*]P (USEPA, 2010) and were expressed as B[*a*]P equivalents (ng/mg PM). The calculated overall carcinogenic potency of the fine and ultrafine PM samples were 1.8 and 1.6 times higher than for the coarse PM. The most important contributions to carcinogenic potential in all size-separated PM samples are B[*a*]P and dibenz[*a,h*]anthracene. In the fine and ultrafine PM samples fluoranthene and cyclopenta[*cd*]pyrene are additional significant contributors.

3.1.4. AhR-mediated activity of extracted fractions

Activation of AhR is a crucial step in the cellular responses to exposure to many environmental pollutants such as PAHs (Barouki et al., 2012). AhR-mediated ("dioxin-like") activities of extracted fractions E1, E2 and E3 from the various road tunnel PM samples were determined in the human AZ-AhR luciferase reporter cell line (Novotna et al., 2011). The results are expressed as pg TCDD equivalents/mg PM in Table 7A. The activities of the extracted fractions did not reach maximal induction of TCDD, however, EC25 and EC50 values as well as TCDD equivalents were calculated. Relatively similar TCDD equivalents were found when comparing the different extracted fractions from the size-separated PM samples. The polar aromatic fractions (E3) were the most potent, followed by the neutral aromatic fractions (E1). The semi-polar aromatic fraction (E2) exerted only a weak AhR-activation.

The AhR-mediated activities of individual PAHs were calculated from the presented chemical data and previously reported induction equivalency factors of individual PAHs in the human transgenic HepG2 model/AZ-AhR cells (Vondráček et al., 2017), and are presented in Table 7B. The most significant contributors to the overall dioxin-like activity were benzo[*k*]fluoranthene, benzo[*j*]fluoranthene and indeno [1,2,3-*cd*]pyrene, while lower contributions of dibenz[*a,h*]anthracene, B[*a*]P and benzo[*b*]fluoranthene were also identified. The fine PM samples with higher concentrations of PAHs with 4- and 5-rings (benz[*a*]anthracene, chrysene, B[*a*]P and benzofluoranthenes], contained slightly higher concentration of TCDD equivalents than the coarse PM and ultrafine samples. However, potent AhR-agonists (benzofluoranthenes, indeno[1,2,3-*cd*]pyrene and dibenz[*a,h*]anthracene)

Table 4
Concentrations of oxy and nitro-PAHs in road tunnel PM.

A. The oxy-PAHs, dinitropyrenes and nitro-oxy-PAHs as well as a number of other polar aromatic compounds are extracted in polar E3 fraction. Concentration of oxy-PAHs in coarse ($PM_{10-2.5}$), fine ($PM_{2.5-0.18}$) and ultrafine ($PM_{0.18}$). PM (ng/mg PM) sampled in a road tunnel and analysed by HPLC. Limit of quantification (LOQ) = 0.01 ng/mg PM

Oxy-PAHs	Coarse PM	Fine PM	Ultrafine PM
1,8-Naphthalic Anhydride	0.17	0.15	0.28
Phenanthrene-9,10-dione	0.02	0.05	0.10
Pyrene-4,5-dione	0.01	0.03	0,05
9H-Fluoren-9-one	0.7	1.4	2.6
Anthrone	2.0	5.8	13.0
Anthracene-9,10-dione (anthraquinone)	0.18	0.47	0.48
7H-Benz[*de*]anthracene-7one (benzanthrone)	0.03	0.26	0.26
9-Hydroxybenzo[*a*]pyrene	0.003	<0.01	<0.01
Benz[*a*]anthracene-7,12-dione	0.01	0.03	0.01
3-Hydroxybenzo[*a*]pyrene	0.09	0.10	0.14
Sum of Oxy-PAHs	*3.1*	*8.2*	*16.9*

B. E2 fractions contain semipolar compounds including all mononitro-PAHs (Ciganek et al., 2004; Pálková et al., 2015). Concentration of nitro-PAHs in coarse, fine and ultrafine PM (ng/mg PM). PM (ng/mg) sampled in a road tunnel and analysed by HPLC

Mono nitrated-PAHs	Coarse PM	Fine PM	Ultrafine PM
1-Nitronaphthalene	<0.01	160	264
2-Nitronaphthalene	<0.01	<0.01	44
2-Nitrofluorene	0.3	1.8	2.6
9-Nitroanthracene	1.6	71	117
3-Nitrophenanthrene	17	<0.01	<0.01
9-Nitrophenanthrene	<0.01	<0.01	<0.01
3-Nitrofluoranthene	<0.01	<0.01	0.1
1-Nitropyrene	0.2	16.2	24.2
2-Nitropyrene	<0.01	0.7	1.1
4-Nitropyrene	<0.01	<0.01	<0.01
6-Nitrochrysene	<0.01	<0.01	<0.01
7-Nitrobenz[*a*]anthracene	<0.01.	<0.01	<0.01
6-Nitrobenzo[*a*]pyrene	<0.01	<0.01	<0.01
Sum of Nitro-PAHs	*19.6*	*249*	*452*

Table 5
Calculated mutagenic potency.

Compound name	Coarse PM	Fine PM	Ultrafine PM
Cyclopenta[*cd*]pyrene	n.d.	3.91	4.64
Benzo[*a*]pyrene	0.38	0.62	0.45
Indeno[1,2,3-*cd*]pyrene	0.10	0.08	0.06
Dibenzo[*a,h*]anthracene	0.01	0.01	0.01
Benzo[*b*]fluoranthene	0.01	0.02	0.04
Benzo[*ghi*]perylene	0.16	0.06	0.03
Benzo[*k*]fluoranthene	0.01	0.02	0.01
Benz[*a*]anthracene	0.01	0.04	0.02
Chrysene	0.00	0.01	0.01
Sum	*0.68*	*4.77*	*5.27*

Mutagenic potency of individual PAHs relative to B[*a*]P were calculated from chemical data presented and mutagenic equivalent factors of PAHs previously published (B[*a*]P eq (ng /mg PM)) (Machala et al., 2001b); n.d., not determined.

Table 6
Calculated carcinogenic potency.

Compound name	Coarse PM	Fine PM	Ultrafine PM
Dibenz[*a,h*]anthracene	0.42	0.40	0.25
Dibenzo[*a,c*]anthracene	n.d.	n.d.	n.d.
Benzo[*a*]pyrene	0.38	0.62	0.45
Benzo[*b*]fluoranthene	0.04	0.07	0.13
Cyclopenta[*cd*]pyrene	n.d.	0.23	0.27
Benzo[*j*]fluoranthene	0.08	0.10	0.07
Benz[*a*]anthracene	0.02	0.10	0.06
Chrysene	0.01	0.08	0.04
Fluoranthene	0.10	0.31	0.39
Indeno[1,2,3-*cd*]pyrene	0.02	0.02	0.01
Benzo[*k*]fluoranthene	<0.01	<0.01	<0.01
Benzo[*ghi*]perylene	0.01	0.00	0.00
Sum	*1.08*	*1.93*	*1.69*

Carcinogenic potency based on carcinogenic equivalents of individual PAHs relative to B[*a*]P (USEPA, 2010) were calculated from chemical data presented (B[*a*]P eq (ng /mg PM)); n.d., not determined.

Table 7
Overall bioassay-derived AhR-activity and calculated AhR- activity of individual PAHs.

A. Canonical AhR-activity of coarse, fine and ultrafine road tunnel PM and their neutral (E1), semi-polar (E2) and polar (E3) extracts determined in HepG2 (human hepatocellular carcinoma cells) stably transfected with AhR-binding sites linked to a luciferase-reporter gene (AZ-AhR cell line).

Sample	mg/mL			pg TCDD/ mg PM
	EC50	EC25	% max	ϕ TEQ
Coarse PM				
E1	5	2	48	38
E2			9	4
E3	4	2	59	58
Fine PM				
E1	5	2	53	47
E2			7	4
E3	3	1	67	53
Ultrafine PM				
E1	6	2	47	38
E2			10	5
E3	4	2	62	49

B. Human AhR-mediated activity (AZ-AhR cells) of selected individual PAHs calculated from presented chemical data and previously reported induction equivalency factors relative to TCDD (Vondráček et al., 2017).

Compound name	Coarse PM	Fine PM	Ultrafine PM
Fluoranthene	n.d.	n.d.	n.d.
Pyrene	n.d.	n.d.	n.d.
Benz[*a*]anthracene	0.005	0.031	0.017
Chrysene	0.011	0.116	0.067
Benzo[*b*]fluoranthene	0.019	0.037	0.067
Benzo[*k*]fluoranthene	0.398	0.653	0.485
Benzo[*a*]pyrene	0.038	0.062	0.044
Dibenz[*a,h*]anthracene	0.072	0.068	0.043
Benzo[*ghi*]perylene	n.d.	n.d.	n.d.
Indeno[1,2,3-*cd*]pyrene	0.408	0.320	0.233
Benzo[*j*]fluoranthene	0.537	0.621	0.480
Sum	*1.486*	*1.907*	*1.436*

n.d. - not detected, induction lower than EC10 of TCDD. AhR-mediated activity of individual PAHs calculated from chemical data and previously reported induction equivalency factors of individual PAHs in human transgenic HepG2 model (Vondráček et al., 2017).

were found in high concentrations on the coarse PM samples. This might explain why the overall calculated AhR-activity of the coarse PM sample is rather similar to that of the fine and ultrafine PM samples, despite lower levels of PAHs.

AhR-mediated activity of the individual PAHs was also calculated from previously reported induction equivalency factors of individual PAHs in *rat hepatoma H4IIE cells,* stably transfected with a luciferase reporter gene under the control of dioxin-responsive enhancers (Machala et al., 2001b). In the rat cellular model, lower AhR-activities were found, compared to the human AZ-AhR model. However, the same major contributors to overall AhR-activity were identified (benzo[*k*]fluoranthene>benzo[*j*]fluoranthene>indeno[1,2,3-*cd*]pyrene>B[*a*]P) (Supplementary Table 2S).

3.2. Inflammatory potential of PM and extracted fractions in human bronchial epithelial cells

Cytotoxicity and pro-inflammatory cytokine responses triggered by the extracted organic fractions E1, E2 and E3 from the coarse and fine PM samples, and their corresponding residual- and parent PM, were examined in the human bronchial epithelial cell line HBEC3-KT. The role of the AhR pathway was assessed by co-treatment with the AhR-inhibitor CH223191. Cells were exposed for 20 h to E1, E2 and E3, and residual PM, all in the concentration equivalent to 100 μg/mL (10.4 μg/cm^2) of parent PM. For the studies on gene expression the same approaches were taken, but exposure periods of 9 and 20 h were chosen. The experimental conditions used were based on optimalization in previous studies (Refsnes et al. submitted 2023). Corresponding studies with organic extracts from ultrafine PM were not possible due to the limited amount of collected sample materials.

3.2.1. Cytotoxicity

Exposure to neutral, semi-polar and polar extracts from the fine or coarse PM samples caused no significant cytotoxicity as measured by the release of LDH (Supplementary Fig. 1S). Slight increases in LDH activity were observed after exposure to the residual PM (PM-EOM) or parent PM, and in particular the parent fine PM (Supplementary Fig. 1S).

3.2.2. Cytokine release

Based on the results from our previous study on road tunnel PM (Skuland et al., 2022), we examined the release of the cytokine IL-1α and the chemokine CXC-motif ligand 8 (CXCL8) to assess the pro-inflammatory responses after exposure to the fractionated organic extracts. In accordance with our previous study (Skuland et al., 2022), both parent PM samples induced significant increases in IL-1α and CXCL8, with the fine PM sample inducing significantly higher responses than the coarse PM sample (Fig. 1). None of the PM extracts from either PM samples increased the release of IL-1α (Fig. 1A). In contrast, the E1 and E3 fractions from both the coarse and fine PM samples increased the release of CXCL8 (Fig. 1B). The residual coarse and fine PM also induced a statistically significant induction of both IL-1α and CXCL8. However, these responses were less than half of those from the respective parent PM (Fig. 1).

The selective AhR-inhibitor CH223191 caused marked and statistically significant reductions in IL-1α and CXCL8 release induced by coarse PM (Fig. 1). CH223191 also inhibited CXCL8 release induced by all three extracts of coarse PM (E1-E3) but did not cause any statistically significant reduction in the cytokine responses induced by the residual coarse PM (Fig. 1A and B). The AhR-inhibitor also appeared to cause a slight reduction in IL-1α and CXCL8 release induced by the fine PM, but this effect was not statistically significant. However, the CXCL8 responses induced by the E1 and E3 extracts of the fine PM were significantly reduced. As for residual coarse PM, the cytokine responses induced by residual fine PM were not significantly affected by CH223191 treatment (Fig. 1A and B).

3.2.3. Gene expression

Expression of the pro-inflammatory genes IL1A, CXCL8 and PTGS2/COX2 in HBEC3-KT cells were examined by qPCR following exposure to

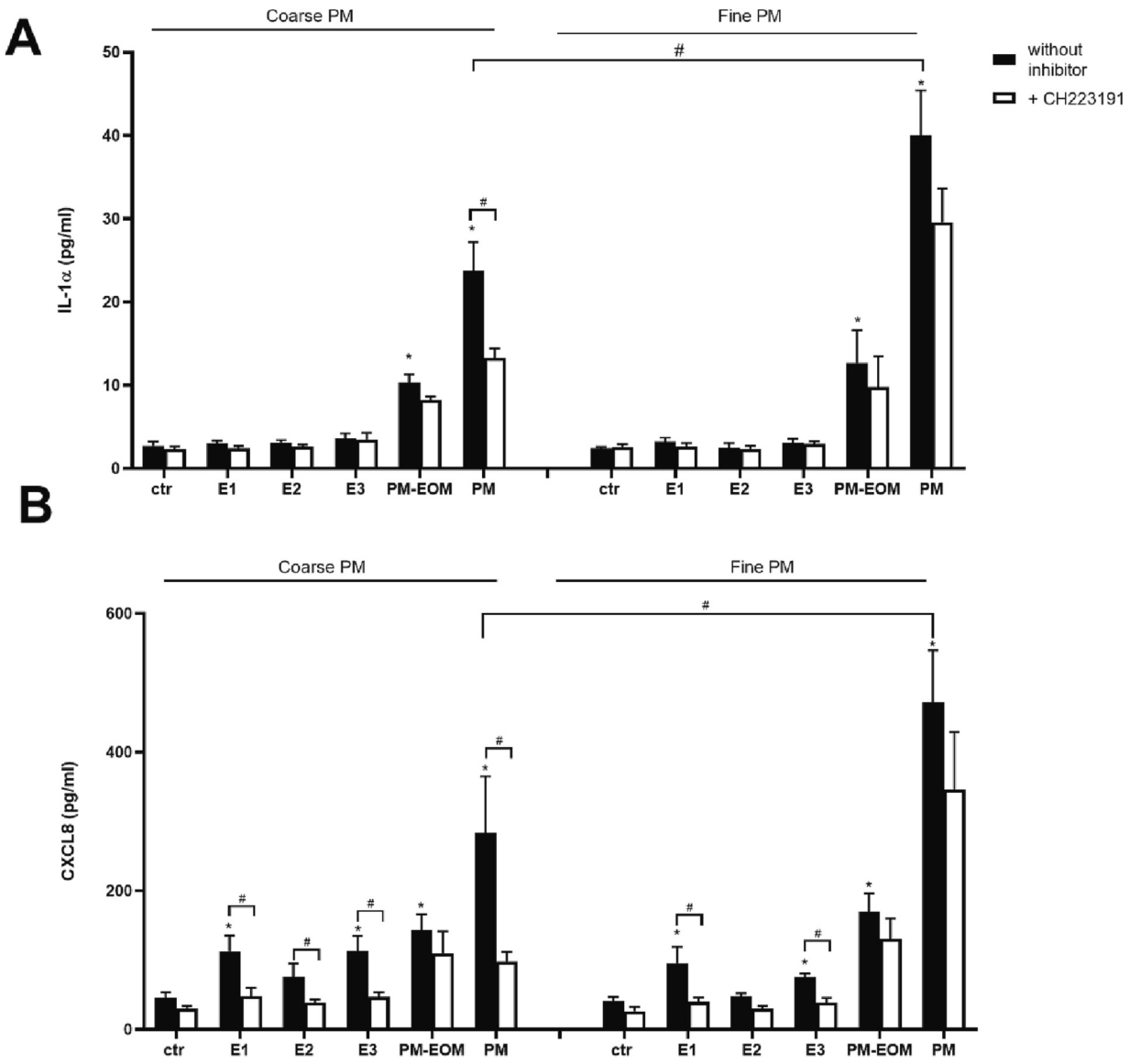

Fig. 1. Pro-inflammatory responses in HBEC3-KT cells exposed to PM extracts, residual PM and parent PM, with or without the AhR-antagonist CH22319. The cells were exposed to neutral (E1), semi-polar (E2) and polar extracts (E3), the residual PM (PM-EOM) or parent PM from coarse ($PM_{10–2.5}$) or fine ($PM_{2.5–0.18}$) PM (equivalent to 100 μg/mL; 10.4 μg/cm^2), for 20 h. The AhR inhibitor CH223191 (1 μM) was added 1 h before start of exposure. Medium was collected and IL-1α (A) and CXCL8 (B) release was measured by ELISA. The data is presented as the mean +/− SEM of 5 independent experiments. Statistical analyses were performed by using two-way ANOVA with Dunnett's Multiple comparison test. *Significantly different from control, # significantly different between groups, $p < 0.05$.

the organic extracts and the residual- and parent PM for 9 and 20 h. Furthermore, the role of AhR was explored by pretreating the cells with the AhR-inhibitor CH223191 (Fig. 2).

The E1 and E3 extracts from both coarse and fine PM, and their corresponding residual and parent PM, induced the expression of IL1A and CXCL8 at 9 or 20 h (Fig. 2A and B). Similar findings were also observed for COX2 (Fig. 2C). An overall evaluation suggests that the parent PM resulted in higher responses than PM-EOM, which were slightly higher than E1 and E2 responses from the corresponding PM. In line with the ELISA results, the fine parent PM apparently induced slightly higher responses than the coarse PM, but this difference was only statistically significant for COX2 after 20 h treatment.

The AhR-inhibitor CH223191 did not cause any statistically significant effects on IL1A, although some reduction in effects were observed, especially for coarse PM and their corresponding extracts (Fig. 2A). However, CH223191 caused a statistically significant inhibition of the CXCL8 expression induced by 20 h exposure to E1 and E3. In line with the ELISA results, the AhR-inhibitor also appeared to reduce CXCL8 expression by the parent coarse PM, but this effect was not statistically significant (Fig. 2B). CH223191 caused a statistically significant reduction in expression of COX2 induced by the parent coarse PM and by the coarse PM E1 extract after 9 h exposure. However, the COX2 expressions induced by all three coarse PM extracts (E1-E3) and the fine PM E1 and E2 extracts were significantly suppressed by the AhR-inhibitor after 20 h exposure (Fig. 2C).

The results on the gene expression of cytochrome P450 1A1 (CYP1A1) and heme oxygenase 1 (HMOX1/HO-1) are presented in Fig. 3. The E1, E2 and E3 extracts from both coarse and fine PM, and their corresponding residual and parent PM, all induced the expression of CYP1A1 at 9 and 20 h (Fig. 3A). Furthermore, the expression of CYP1A1 induced by the residual PM was low compared to the parent coarse and fine PM, and lower or similar to the extracts. As expected, the AhR-inhibitor CH223191 markedly suppressed CYP1A1 by all exposures (Fig. 3A). The gene expression of HO-1 was induced after exposure to the coarse and fine residual and parent PM at both time points (Fig. 3B). The fine parent PM induced significantly higher HO-1 expression than the

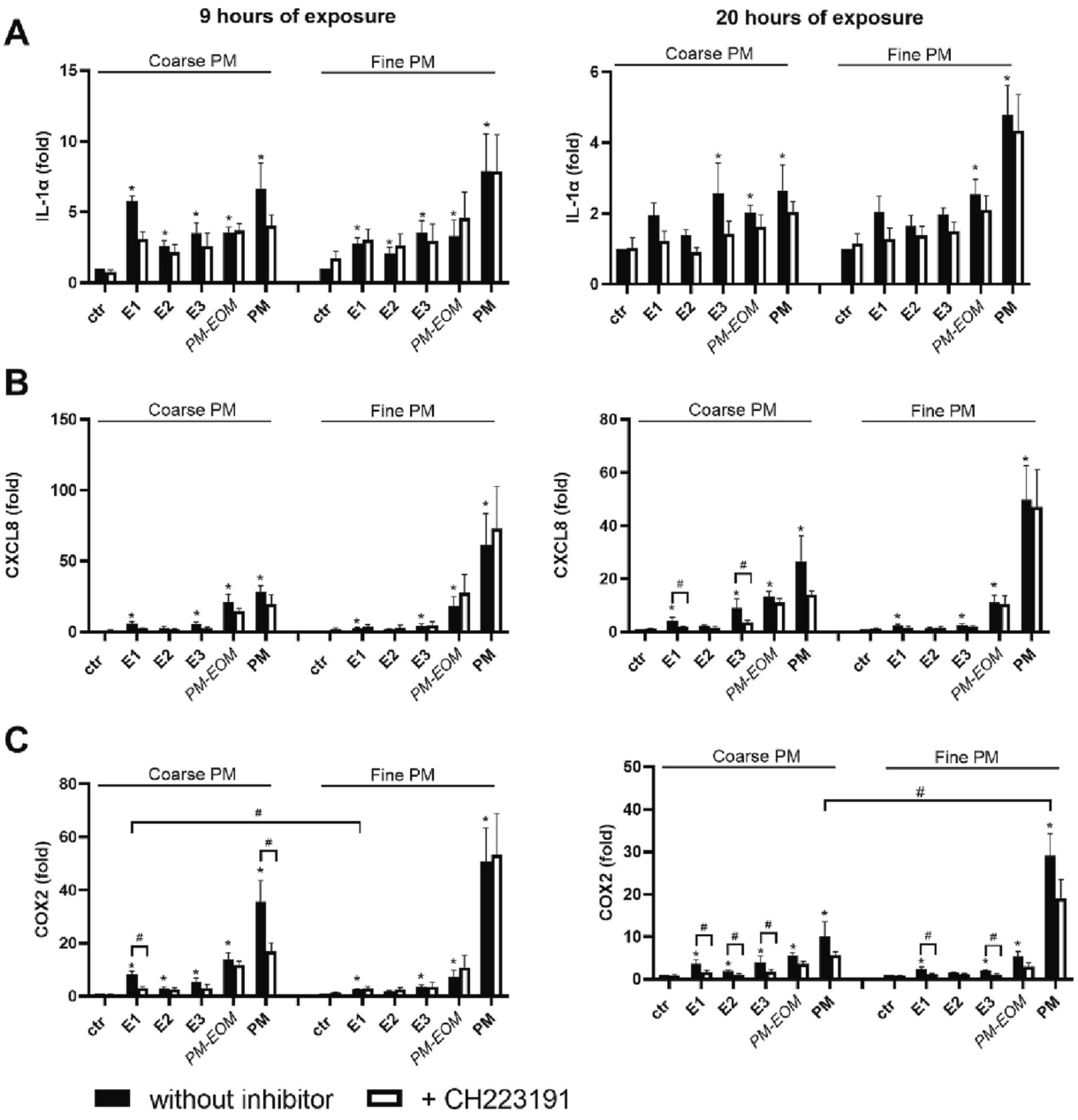

Fig. 2. The gene expression of cytokines and COX2 in HBEC3-KT cells exposed to PM extracts, residual PM and parent PM, with or without the AhR-antagonist CH223191. The cells were exposed to neutral (E1), semi-polar (E2) and polar extracts (E3), the residual PM (PM-EOM) or parent PM from coarse ($PM_{10–2.5}$) or fine ($PM_{2.5–0.18}$) PM (equivalent to 100 μg/mL; 10.4 μg/cm^2). The AhR inhibitor CH223191 (1 μM) was added 1 h before start of exposure. After 9 h and 20 h exposure cells were collected. The gene expressions of IL1A (A), CXCL8 (B) and COX2 (C) were analysed by qPCR. The data is presented as the mean +/− SEM of 4 independent experiments. Statistical analyses were performed by using two-way ANOVA with Dunnett's Multiple comparison test. *Significantly different from control, # significantly different between groups, $p < 0.05$.

coarse PM sample. No effects were seen after exposure to any of the extracts of either size fraction. However, while the coarse residual PM was almost identical after extraction, fine residual PM induced less than half the response of parent fine PM after both 9 and 20 h exposure. The AhR inhibitor had no effect on the expression of HO-1 (Fig. 3B).

4. Discussion

Several biological responses linked to exposure of ambient PM may contribute to development and/or exacerbation of non-malignant and malignant respiratory effects. These responses have been attributed to various properties of the PM, including shape, size, and surface reactivity, as well as to the chemical compounds adsorbed on the particles. Road tunnels represent a useful environment for sampling traffic-derived PM due to minimal contribution from non-traffic sources. Here we report the occurrence of various metals in PM, several of which some have been reported to induce pro-inflammatory and health-related responses. Furthermore, we characterized the PM samples with respect to the levels of US EPA PAHs, other PAHs, and PAH derivatives in extracts from coarse, fine and ultrafine PM, and calculated the theoretical mutagenic and carcinogenic potency and AhR-mediated activity of the individual PAHs. Finally, we performed in vitro bioassays focused on AhR-mediated activity and pro-inflammatory responses after exposure to chromatographic fractions of size-separated PM.

During the last years, chemical characterization of potentially toxic metals or elements in airborne particles has become an important part of

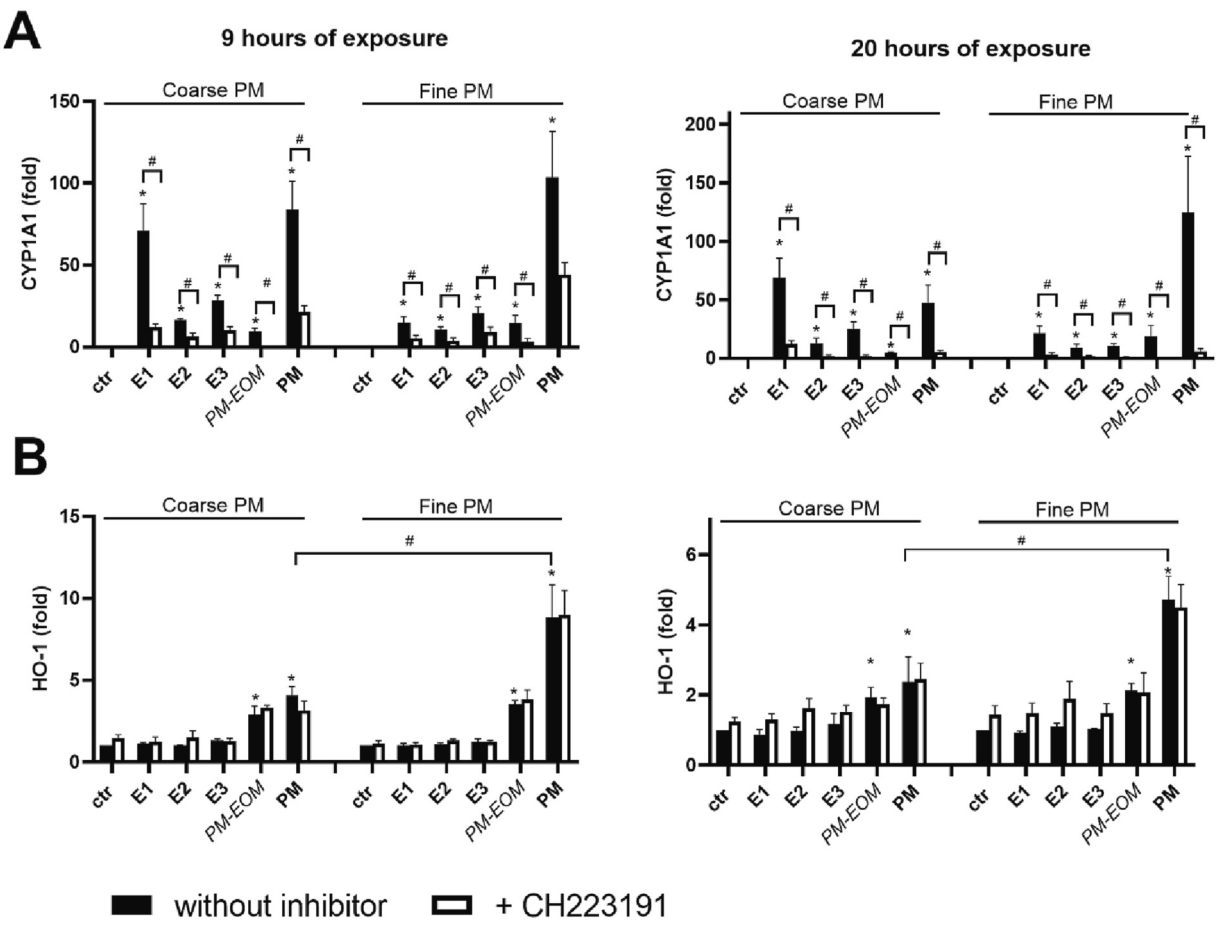

Fig. 3. The gene expression of CYP1A1 and HO-1 in HBEC3-KT cells exposed to PM extracts, residual PM and parent PM, with or without the AhR-antagonist CH223191. The cells were exposed to neutral (E1), semi-polar(E2) and polar extracts (E3) from coarse ($PM_{10–2.5}$) or fine ($PM_{2.5–0.18}$) PM, the residual PM (PM-EOM) or parent PM (equivalent to 100 μg/mL; 10.4 μg/cm^2) for 9 h and 20 h. The AhR-inhibitor CH223191 (1 μM) was added 1 h before start of exposure. The gene expression of CYP1A1 (A) and HO-1 (B) was analysed by qPCR. The data is presented as the mean +/− SEM of 4 independent experiments. Statistical analyses were performed by using two-way ANOVA with Dunnett's Multiple comparison test. *Significantly different from control, # significantly different between groups, $p < 0.05$.

studies on air pollution and human health risk linked to toxicity and/or carcinogenicity (Świetlik and Trojanowska, 2022). The release of elements from traffic suggests contribution from different sources such as combustion of fuel and wear of road pavement, brakes and tires (Miler, 2021; Zhou et al., 2021). Interestingly, the fine PM sample, which induced the highest pro-inflammatory responses in this and our previous study, contained the highest levels of Cu, Mo, Sn and Ba, suggesting that metals could be a potential contributor to the observed differences. The various levels of the redox-active transition metal Cu could be a possible contributor to these differences. However, there are still no established equivalency factors for metal toxicity and pro-inflammatory effects. The subject is complex, as the particle toxicity and pro-inflammatory potential may be linked both to metals at the particle surface as well to the metal ions released from the particles. Regardless, it is interesting to note the occurrence of Zn and Mn, metals reported to induce adverse health effects following inhalation (Świetlik and Trojanowska, 2022) and pro-inflammatory responses in lung cells (Låg et al., 2016; Shao et al., 2018). It is also notable that the residual particles after extraction of organic chemicals still have pro-inflammatory potential, which may indicate a role for metals on the particle surface.

PAHs are considered an important contributor to the effects of ambient PM (Kermani et al., 2021). A larger proportion of the combustion PAHs is bound to PM during winter compared to summer (Gualtieri et al., 2010), as more volatile PAHs will condensate on particles due to lower temperatures. Similarly, as the temperature during summer within road tunnels is lower than outside, higher concentrations of PAHs in PM samples are often found inside tunnels (Wingfors et al., 2001). However, in the present study we find that the total amount of PAHs on road tunnel PM was at least one order of magnitude lower than that e.g. reported in urban winter air PMs from Milan (Gualtieri et al., 2010) and residential districts of Ostrava-Radvanice and Bartovice, the most polluted industrial sites in the Czech Republic (Topinka et al., 2015). Notably, the average temperature (14.9 °C) in the tunnel used in the present study is rather high. Furthermore, during recent years the prevalence of cars using new filters, engine technology, and other types of fuel, as well as the number of electric vehicles, has increased substantially in Norway. Thus, the reason for the lower levels of PAHs in our PM samples could be due to less emission of PAHs per mass of PM from the current vehicle fleet in Norway. In addition, the PM samples characterized in previous studies from Italy and the Czeck Republic were sampled in urban areas during winter season, likely with lower temperatures in addition to contributions from other sources than traffic, such as industry and residential wood combustion.

PAHs on traffic PM may also result from other sources than from exhaust emissions. Notably, the use of studded tires in the winter season in Norway will result in large amounts of PM from road pavement, including bitumen. Accordingly, it is interesting to note that although more US EPA PAHs were found in ultrafine and fine versus coarse samples, high accumulation of the high-molecular-weight PAHs benzo [*ghi*]perylene, indeno[1,2,3-*cd*]pyrene and coronene was found in

coarse PM, suggesting a substantial contribution from other primary non-combustion sources, such as bitumen and tires. In contrast, the occurrence of lower MW PAHs (2-, 3- and 4-rings PAHs) in the coarse PM samples are more probably due to secondary condensation. Aggregation of ultrafine PM is less likely as this will not significantly contribute to the mass of the coarse PM (Skuland et al., 2022).

The relative pattern of PAHs, and their oxygenated (oxy-PAHs) and nitrated (nitro-PAHs) derivatives in the PM samples is mostly in agreement with observations previously reported in road tunnels (Keyte et al., 2016; Wingfors et al., 2001). In line with previous studies (Gualtieri et al., 2010; Wingfors et al., 2001), most of the particle-associated PAHs were found in the fine and ultrafine PM. Notably, the oxy-PAHs and mononitro-PAHs accumulated mainly in the fine and ultrafine PM samples. Anthrone, 9H-fluoren-9-one and anthracene-9,10-dione were the most abundant oxy-PAHs in the road tunnel PM. While both oxy- and nitro-PAHs may be formed through atmospheric reactions, certain nitro-PAHs such as 1-nitropyrene almost exclusively derive directly from diesel engine emissions (Anders Feilberg and TorbenNielsen, 2001; IARC, 2014). Based on analysis of urban and rural air samples (Anders Feilberg and TorbenNielsen, 2001), it can be assumed that 9-nitroanthracene also derived directly from diesel exhaust. Notably, much higher concentrations of these two mononitro-PAHs were observed in the ultrafine and fine PM, compared to coarse PM. Furthermore, 1-nitropyrene is almost exclusively found bound to primary combustion particles and very little is emitted in the gas phase (IARC, 2014). This suggests that there is a high content of primary exhaust particle components in the ultrafine PM, somewhat less in the fine PM, and very little in the coarse PM. Notably, the distribution of the three most abundant mononitro-PAHs (1-nitronaphtalene, 9-nitroanthracene and 1-nitropyrene) in the fine versus ultrafine PM, indicates that around 60% of the mass of fine PM may consist of agglomerated ultrafine PM. It also underscores that coarse PM contained very little primary particles from exhaust emissions and that the PAH content from this size fraction was more likely derived from other sources, as previously discussed.

IARC has classified diesel exhaust, PM in ambient air, and B[*a*]P as carcinogenic (IARC, 2014; IARC, 2016). PM may also trigger inflammation, which is a central process in cancer. Carcinogenic metals and PAHs are likely to contribute to PM toxicity via DNA damage, inflammation and other mechanisms. Despite their structural similarities, PAHs vary greatly in their mutagenic and carcinogenic effects, with some PAHs classified as possible (Group 2B), probable (Group 2A) or human (Group 1) carcinogens by IARC (IARC, 2010). Mechanisms explaining the carcinogenicity of the model PAH B[*a*]P include the formation of reactive electrophiles and redox-active metabolites, causing DNA damage and mutations. Some PAHs may contribute to carcinogenicity by non-genotoxic mechanisms, such as altering DNA repair and causing genome instability, increasing cell proliferation and/or inhibiting apoptosis, reducing contact inhibition, inducing epithelial mesenchymal transition, modulating inflammation, and increasing the migration of cancer cells (Goodson 3rd et al., 2015; IARC, 2010; IARC, 2014; IARC, 2016; Nahta et al., 2015; Nemmar et al., 2013). Besides modulating the generation of reactive electrophilic metabolites, AhR-ligandation may change the expression of genes linked to other key events in toxicity and carcinogenicity of PAHs (Boström et al., 2002). The role of AhR in carcinogenicity via inflammation is complex (Øvrevik et al., 2014). It is not necessarily linked to gene expression, but possibly also to rapid non-genomic responses, including calcium signaling (Ca^{2+}) (Brinchmann et al., 2018). Notably, the relative importance of various PAH ligands for non-genomic AhR-signaling may differ from that linked to AhR-mediated gene expression (Brinchmann et al., 2018). Due to this complexity, it is still a challenge to integrate identified carcinogens in ambient PM samples with toxicological knowledge from experimental studies into cancer risk and impact on assessment.

There are several approaches for the assessment of the toxic potencies of particles in urban air. These are often based on in vitro assays for genotoxicity, mutagenicity, cellular transformation and tumor promoting capacity (e.g. inhibition of gap junction intracellular communication, AhR-activity or inflammatory potential) (Nahta et al., 2015; Nemmar et al., 2013). The whole particles or their extracts may be used for testing the overall toxic potency. Alternatively, one can estimate PM toxicity by combining measured levels of specific chemicals in PM with information of their toxic potency from animal or in vitro experiments (Machala et al., 2001b; Vondráček et al., 2017). All this information is relevant when elucidating how PM may induce cancer, but the different parameters do not necessarily correlate to each other. Thus, in the present study, we discuss information regarding PAHs linked to mutagenicity, carcinogenic potencies, AhR-activity, and inflammation separately.

The calculated mutagenic and carcinogenic activities of the size-separated PM samples based on PAHs potency were somewhat lower for the coarse sample than the fine and ultrafine PM. Cyclopenta[*cd*]pyrene was the most prominent contributor to the estimated mutagenicity of the individual PAHs found in the fine and ultrafine PM samples, followed by B[*a*]P. Cyclopenta[*cd*]pyrene is regarded as a significant contributor to the total mass of biologically active, particle-associated PAHs in emissions from diesel vehicles (Tong and Karasek, 1984; Westerholm et al., 1991). Moreover, it is reported to be a potent genotoxic mutagen in experimental settings and a carcinogen in mice (Beach and Gupta, 1994; Nesnow et al., 1994). The mutagenic potency calculated from relative mutagenicity equivalency factors and measured levels of PAHs and PAH-derivatives (ΣBaP_{MEQ}) found in the fine and ultrafine PM samples was 7- and 8-times higher than in the coarse PM sample. These estimated findings are in line with a higher genotoxicity potential of fine versus coarse PM previously reported in human lung cells (Hornberg et al., 1998; Velali et al., 2016). However, in a previous study we found the presence of double-stranded DNA breaks to be similar between all size-separated urban air PM sampled during winter (Longhin et al., 2013). Nevertheless, no such effect was induced by corresponding summer PM samples which had ten times lower PAH content, supporting a role for PAHs. Others have also reported similar ΣBaP_{MEQ} between fine and coarse urban air PM, and a higher PAH-related mutagenic potency during winter season (Manoli et al., 2016). The relative differences of mutagenicity between size-separated PM observed in our study compared to others may be due to different PAH-profiles, contribution from other chemicals besides the PAHs, and/or that different "mutagenic endpoints" were measured.

Most studies of the carcinogenic potency of urban airborne PAHs use PM samples with different particle sizes, in which the PAHs may come from multiple sources. Mobile sources including working machinery and, in some countries, residential wood combustion, have been identified as the most important local sources responsible for urban concentrations of PAHs (Boström et al., 2002; Gianelle et al., 2013). In the present study, we find that the estimated carcinogenicity of the fine and ultrafine PM, based on levels of carcinogenic PAHs (PAH-related carcinogenic potency of particles, ΣBaP_{CEQ}) was 1.8 and 1.6 times higher than for the coarse PM, thus more similar than the mutagenic potency. This may partly be explained by the fact that the contributing carcinogenic PAHs B[*a*]P and dibenz[*a,h*]anthracene are found in all size-separated PM. Interestingly, low molecular PAH fluoranthene also contributed significantly to the total carcinogenic potency. The estimated carcinogenic (ΣBaP_{CEQ}) potency of coarse and fine PM from combined urban sources has previously been reported to be rather equal (Manoli et al., 2016; Pehnec and Jakovljević, 2018), and B[*a*]P has been found to be a good indicator for toxic PAHs at least in the cold season (Belis et al., 2011).

AhR-activity were assessed by the human AZ-AhR model with multiple DRE-elements upstream of a luciferase reporter gene (Novotna et al., 2011). AhR-inducing activities of the ultrafine and coarse PM samples were only slightly lower than for the fine sample. The polar aromatic fractions (E3) were most potent regarding AhR-activity, followed by the neutral aromatic fractions (E1), while the semi-polar aromatic fraction (E2) exerted only a weak activation in this cell line. In

accordance with our previous studies (Vondráček et al., 2017), complex neutral aromatic and polar aromatic fractions showed significantly higher AhR- activity compared to the sum of chemically calculated equivalents of individual PAHs or oxy-PAHs. Thus, a large part of the overall AhR-mediated activity was not explained by the presence of polycyclic aromatic AhR-agonists. Furthermore, AZ-AhR-activity of corresponding extracts from coarse, fine and ultrafine road tunnel PM were rather similar, despite large differences in the qualitative and quantitative PAHs pattern analysed in the various size-separated PM samples. The reason(s) for this phenomenon(s) remains to be elucidated, but presence of various polychlorinated aromatic compounds with AhR-activities might be a possible explanation.

In the case of polar aromatic E3 fraction, major oxy-PAHs (9-fluorenone, anthrone, anthraquinone, benzanthrone and benz[*a*]anthracene-7,12-dione) previously identified in environmental samples have been reported to elicit only a weak in vitro AhR-mediated activity. Their induction equivalency factors have been shown to be approximately three orders of magnitude lower than those of B[*a*]P (Machala et al., 2001b). Therefore, the contribution of these oxy-PAHs to the overall AhR-mediated activity in the polar E3 fraction would be expected to be relatively low. However, some other oxy-PAHs might be responsible for the potent AhR-activation (Misaki et al., 2007; Vondráček et al., 2017; Wincent et al., 2016). As previous studies have not identified major aromatic agonists of the AhR that would be present in the polar fraction, more attention should be paid to the identification of polar polyaromatic agonists interacting with this receptor.

Further analysis of AhR-activity, measured as CYP1A1 gene expression in HBEC3-KT cells, mostly supported rather similar responses induced by the coarse and fine PM. However, in contrast to the AZ-AhR reporter gene assay, the E1 extract in general induced higher CYP1A1 expression than E2 and E3, in line with what would be expected based on the high content of unsubstituted AhR-activating PAHs in E1 fractions. The lack of correlation between the high AhR-mediated activity by the polar E3 fraction identified in the reporter gene assay and the low induction of CYP1A1 mRNA in HBEC-3KT cells could be linked to different cell models and endpoints being used. Alternatively, AhR-independent, sub-toxic effects of compounds within E3 fraction might have limited the induction of CYP1A1 in the HBEC3-KT cells, while the liver hepatoma cells used in the reporter gene assay could be less sensitive to their toxic action.

The present study shows that exposure to the fine and coarse road tunnel PM samples induced several genes/proteins related to pro-inflammatory potential. The results are in accordance with our previous study and suggest that the pro-inflammatory potential of the PM samples was related to the ratio of OC to total PM mass (Skuland et al., 2022). Exposure to both PM samples, as well as their neutral aromatic fractions (E1) and polar (E3) fractions increased the release of CXCL8, while IL-1α was induced only after exposure to the 2 PM samples. On the other hand, the E1 and E3 extracts from both coarse and fine PM and their corresponding residual and parent PM increased the gene expression of IL1A and CXCL8 at 9 and/or 20 h. This indicate that some of the extracted compounds from PM may inhibit the synthesis and/or translocation of IL-1α protein.

PAHs have been reported to modulate immune responses via the AhR link (O'Driscoll et al., 2018; Quintana et al., 2008), including the pro-inflammatory responses induced by diesel exhaust particles in human lung epithelial cells (Øvrevik et al., 2014; Øvrevik et al., 2017). Recently, we found that the chemical AhR-inhibitor CH223191 markedly reduced the release and expression of CXCL8 in HBEC3-KT induced by coarse, fine and ultrafine road tunnel PM, supporting a role for PAHs via AhR (Refsnes et al. submitted 2023). This is confirmed by the present study and extended by the results of experiments using the extracted fractions of the PM samples. Notably, the effects of the fine PM and the corresponding extracts were less affected by CH223191 than the particles and extracts from the coarse PM sample. The partial inhibition seen by CH223191 may indicate ligand selective effects, and that CH223191 does not fully inhibit all AhR-dependent activity induced by the fine PM. However, it could also be that some additional AhR-independent mechanisms are important for the fine PM responses in the present study. Overall, the E1 and E3 fractions were somewhat more potent than E2 with regard to mRNA expression and release of cytokines. The residual PM had some pro-inflammatory activity, which seemed to be mediated via AhR-independent mechanisms.

In our previous study, pre-treatment of HBEC3-KT with the antioxidant *N*-acetylcysteine reduced the tunnel PM-induced expression of COX2 and expression and release of CXCL8 and IL1A/IL-1α, suggesting a role for ROS in the cellular signaling processes (Refsnes et al. submitted 2023). This is supported by increased production of HO-1, which is linked to the redox-sensitive transcription factor nuclear factor erythroid–related factor 2 (Nrf2) (Ryter et al., 2006). Taken together, we found significant contribution of particles to the induced gene expression and release of IL1A/IL-1α and CXCL8, as well as induction of COX2 and HO-1. The AhR-inhibitor partly suppressed the expression and release of pro-inflammatory genes/proteins, indicating a corresponding role of AhR. Thus, crucial constituents in the road tunnel PM with regard to pro-inflammatory responses likely include, parent PAHs, metabolised PAHs and oxy-PAHs, but also other organic compounds in the OC-fraction as well as metals may be involved in the process.

In conclusion, the calculated mutagenic and carcinogenic activity of coarse, fine and ultrafine PM from a road tunnel, based on PAHs potency, suggested that coarse PM was somewhat less potent than fine and ultrafine PM. However, the measured AhR-activities of the PM samples were more similar. The pro-inflammatory responses to fine PM exposure were somewhat higher than the effects of coarse PM. The results suggest a role for both metals and AhR-activity in the pro-inflammatory responses. Possible candidates include PAHs and oxy-PAHs, but substantial pro-inflammatory contributions from other chemicals, as well as for metals, are likely.

Declarations

Ethics for approval and consent to participate, Not Applicable. Consent for publication, Not Applicable.

Author contributions

TS performed all experiments and contributed to all experimental planning and design with HBEC3K cells in collaboration with ML, VSG, JAH, JO and MR at NIPH. RBJ coordinated collection of PM. EM and ML coordinated measure and analysis of elements. Fractionation of PM extracts was performed by MC and JN, PAHs and PAH-derivatives were measured by JN and MP, AhR-mediated activity by KP; corresponding analyses and calculated mutagenic, carcinogenic and AhR-mediated potencies by MC and MM. TS performed the analysis and statistics of cellular effects. JAH drafted the first version of the manuscript, all authors were involved in writing the final version of the manuscript with JAH, ML, TS, VSG, ES, JO, MR, and MM as main responsible. All authors read, commented, and approved the final manuscript.

Funding

The work was performed as part of the PrevenTAP-project funded by the Research Council of Norway, through the Better Health-program (Grant no. 260381). The work was also supported by the Czech Science Foundation (project no. 21-00533S).

Declaration of Competing Interest

The authors declare that they have no competing interests. The authors alone are responsible for the content and writing of the paper.

Data availability

Data will be made available on request.

Acknowledgements

We thank Daan L A C Leseman and Flemming R Cassee, National Institute for Public Health and the Environment - RIVM, PO Box 1, 3720 BA, Bilthoven, The Netherlands, for analysis of ROS; Jessica Emond and Alena Kubátová, Department of Chemistry, University of North Dakota, Grand Forks, ND, USA for OC/EC analysis. The metal analyses were purchased by NILU; Norwegian Institute of Air Research (NILU), 2007, Kjeller, Norway. The description of method for metal analysis was quality assured by Dr. Hilde Uggerud from NILU.

Appendix A. Supplementary data

Supplementary data to this article can be found online at https://doi.org/10.1016/j.tiv.2023.105611.

References

Anders Feilberg, M.W.P., TorbenNielsen, Henrik Skov, 2001. Occurrence and sources of particulate nitro-polycyclic aromatic hydrocarbons in ambient air in Denmark. Atmos. Environ. 35 (2), 353–366.

Andersson, J.T., Achten, C., 2015. Time to say goodbye to the 16 EPA PAHs? Toward an up-to-date use of PACs for environmental purposes. Polycycl. Aromat. Compd. 35 (2–4), 330–354. https://doi.org/10.1080/10406638.2014.991042.

Andrysík, Z., Vondráček, J., Marvanová, S., et al., 2011. Activation of the aryl hydrocarbon receptor is the major toxic mode of action of an organic extract of a reference urban dust particulate matter mixture: the role of polycyclic aromatic hydrocarbons. Mutat. Res. 714 (1–2), 53–62. https://doi.org/10.1016/j.mrfmmm.2011.06.011.

Barouki, R., Aggerbeck, M., Aggerbeck, L., Coumoul, X., 2012. The aryl hydrocarbon receptor system. Drug Metabol. Drug Interact. 27 (1), 3–8. https://doi.org/10.1515/dmdi-2011-0035.

Beach, A.C., Gupta, R.C., 1994. DNA adducts of the ubiquitous environmental contaminant cyclopenta[cd]pyrene. Carcinogenesis 15 (5), 1065–1072. https://doi.org/10.1093/carcin/15.5.1065.

Belis, C.A.C.J., Duane, M., Forcina, V., Pedroni, V., Passarella, R., Tanet, G., Douglas, K., Piazzalunga, A., Bolzacchini, E., Sangiorgi, G., Perrone, M.-G., Ferrero, L., Fermo, P., Larsen, B.R., 2011. Sources for PM air pollution in the Po Plain, Italy: I. Critical comparison of methods for estimating biomass burning contributions to benzo(a) pyrene. Atmos. Environ. 45 (39), 7266–7275.

Borm, P.J.A., Lison, D., Driscoll, K., et al., 2022. Inflammation as a key outcome pathway in particle induced effects in the lung. Front. Public Health 10, 869041. https://doi.org/10.3389/fpubh.2022.869041.

Boström, C.E., Gerde, P., Hanberg, A., et al., 2002. Cancer risk assessment, indicators, and guidelines for polycyclic aromatic hydrocarbons in the ambient air. Environ. Health Perspect. 110 (Suppl. 3), 451–488. https://doi.org/10.1289/ehp.110-1241197.

Brinchmann, B.C., Le Ferrec, E., Bisson, W.H., et al., 2018. Evidence of selective activation of aryl hydrocarbon receptor nongenomic calcium signaling by pyrene. Biochem. Pharmacol. 158, 1–12. https://doi.org/10.1016/j.bcp.2018.09.023.

Campbell, S.J., Utinger, B., Lienhard, D.M., et al., 2019. Development of a physiologically relevant online chemical assay to quantify aerosol oxidative potential. Anal. Chem. 91 (20), 13088–13095. https://doi.org/10.1021/acs.analchem.9b03282.

Cassee, F.R., Héroux, M.E., Gerlofs-Nijland, M.E., Kelly, F.J., 2013. Particulate matter beyond mass: recent health evidence on the role of fractions, chemical constituents and sources of emission. Inhal. Toxicol. 25 (14), 802–812. https://doi.org/10.3109/08958378.2013.850127.

Chen, L.C., Lippmann, M., 2009. Effects of metals within ambient air particulate matter (PM) on human health. Inhal. Toxicol. 21 (1), 1–31. https://doi.org/10.1080/08958370802105405.

Ciganek, M., Neca, J., Adamec, V., Janosek, J., Machala, M., 2004. A combined chemical and bioassay analysis of traffic-emitted polycyclic aromatic hydrocarbons. Sci. Total Environ. 334-335, 141–148. https://doi.org/10.1016/j.scitotenv.2004.04.034.

Dominski, F.H., Lorenzetti Branco, J.H., Buonanno, G., Stabile, L., Gameiro da Silva, M., Andrade, A., 2021. Effects of air pollution on health: a mapping review of systematic reviews and meta-analyses. Environ. Res. 201, 111487 https://doi.org/10.1016/j.envres.2021.111487.

Durant, J.L., Busby Jr., W.F., Lafleur, A.L., Penman, B.W., Crespi, C.L., 1996. Human cell mutagenicity of oxygenated, nitrated and unsubstituted polycyclic aromatic hydrocarbons associated with urban aerosols. Mutat. Res. 371 (3–4), 123–157. https://doi.org/10.1016/s0165-1218(96)90103-2.

Durant, J.L., Lafleur, A.L., Busby Jr., W.F., Donhoffner, L.L., Penman, B.W., Crespi, C.L., 1999. Mutagenicity of C24H14 PAH in human cells expressing CYP1A1. Mutat. Res. 446 (1), 1–14. https://doi.org/10.1016/s1383-5718(99)00135-7.

Gianelle, V.C.C., Caserini, S., Ozgen, S., Galante, S., Marongiu, A., Lanzani, G., 2013. Benzo(a)pyrene air concentrations and emission inventory in Lombardy region, Italy. Atmos. Pollut. Res. 4, 257–266.

Goodson 3rd, W.H., Lowe, L., Carpenter, D.O., et al., 2015. Assessing the carcinogenic potential of low-dose exposures to chemical mixtures in the environment: the challenge ahead. Carcinogenesis 36 (Suppl. 1), S254–S296. https://doi.org/10.1093/carcin/bgv039.

Gualtieri, M., Øvrevik, J., Holme, J.A., et al., 2010. Differences in cytotoxicity versus pro-inflammatory potency of different PM fractions in human epithelial lung cells. Toxicol. in Vitro 24 (1), 29–39. https://doi.org/10.1016/j.tiv.2009.09.013.

Hornberg, C., Maciuleviciute, L., Seemayer, N.H., Kainka, E., 1998. Induction of sister chromatid exchanges (SCE) in human tracheal epithelial cells by the fractions PM-10 and PM-2.5 of airborne particulates. Toxicol. Lett. 96-97, 215–220. https://doi.org/10.1016/s0378-4274(98)00075-7.

IARC, 2010. Some non-heterocyclic polycyclic aromatic hydrocarbons and some related occupational exposures. In: Working Group on the Evaluation of Carcinogenic Risk to Humans. IARC Press, Lyon, France.

IARC, 2013. Some chemicals present in industrial and consumer products, food and drinking-water. IARC Monogr. Eval. Carcinog. Risks Hum. 101, 9–549.

IARC, 2014. Diesel and gasoline engine exhausts and some nitroarenes. IARC monographs on the evaluation of carcinogenic risks to humans. IARC Monogr. Eval. Carcinog. Risks Hum. 105, 9–699.

IARC, 2016. Outdoor air pollution. IARC Monogr. Eval. Carcinog. Risks Hum. 109, 9–444.

Ishihara, Y., Kado, S.Y., Hoeper, C., Harel, S., Vogel, C.F.A., 2019. Role of NF-kB RelB in aryl hydrocarbon receptor-mediated ligand specific effects. Int. J. Mol. Sci. 20 (11) https://doi.org/10.3390/ijms20112652.

Kermani, M., Rahmatinia, T., Oskoei, V., et al., 2021. Potential cytotoxicity of trace elements and polycyclic aromatic hydrocarbons bounded to particulate matter: a review on in vitro studies on human lung epithelial cells. Environ. Sci. Pollut. Res. Int. 28 (40), 55888–55904. https://doi.org/10.1007/s11356-021-16306-y.

Keyte, I.J., Albinet, A., Harrison, R.M., 2016. On-road traffic emissions of polycyclic aromatic hydrocarbons and their oxy- and nitro- derivative compounds measured in road tunnel environments. Sci. Total Environ. 566-567, 1131–1142. https://doi.org/10.1016/j.scitotenv.2016.05.152.

Låg, M., Øvrevik, J., Totlandsdal, A.I., et al., 2016. Air pollution-related metals induce differential cytokine responses in bronchial epithelial cells. Toxicol. in Vitro 36, 53–65. https://doi.org/10.1016/j.tiv.2016.07.004.

Låg, M., Rodionov, D., Øvrevik, J., Bakke, O., Schwarze, P.E., Refsnes, M., 2010. Cadmium-induced inflammatory responses in cells relevant for lung toxicity: expression and release of cytokines in fibroblasts, epithelial cells and macrophages. Toxicol. Lett. 193 (3), 252–260. https://doi.org/10.1016/j.toxlet.2010.01.015.

Låg, M., Skuland, T., Godymchuk, A., Nguyen, T.H.T., Pham, H.L.T., Refsnes, M., 2018. Silica nanoparticle-induced cytokine responses in BEAS-2B and HBEC3-KT cells: significance of particle size and signalling pathways in different lung cell cultures. Basic Clin. Pharmacol. Toxicol. 122 (6), 620–632. https://doi.org/10.1111/bcpt.12963.

Låg, M., Øvrevik, J., Refsnes, M., Holme, J.A., 2020. Potential role of polycyclic aromatic hydrocarbons in air pollution-induced non-malignant respiratory diseases. Respir. Res. 21 (1), 299. https://doi.org/10.1186/s12931-020-01563-1.

Longhin, E., Pezzolato, E., Mantecca, P., et al., 2013. Season linked responses to fine and quasi-ultrafine Milan PM in cultured cells. Toxicol. in Vitro 27 (2), 551–559. https://doi.org/10.1016/j.tiv.2012.10.018.

Machala, M., Ciganek, M., Bláha, L., Minksová, K., Vondrácк, J., 2001a. Aryl hydrocarbon receptor-mediated and estrogenic activities of oxygenated polycyclic aromatic hydrocarbons and azaarenes originally identified in extracts of river sediments. Environ. Toxicol. Chem. 20 (12), 2736–2743.

Machala, M., Vondrácek, J., Bláha, L., Ciganek, M., Neca, J.V., 2001b. Aryl hydrocarbon receptor-mediated activity of mutagenic polycyclic aromatic hydrocarbons determined using in vitro reporter gene assay. Mutat. Res. 497 (1–2), 49–62. https://doi.org/10.1016/s1383-5718(01)00240-6.

Manoli, E., Kouras, A., Karagkiozidou, O., Argyropoulos, G., Voutsa, D., Samara, C., 2016. Polycyclic aromatic hydrocarbons (PAHs) at traffic and urban background sites of northern Greece: source apportionment of ambient PAH levels and PAH-induced lung cancer risk. Environ. Sci. Pollut. Res. Int. 23 (4), 3556–3568. https://doi.org/10.1007/s11356-015-5573-5.

Miler, M., 2021. Airborne particles in city bus: concentrations, sources and simulated pulmonary solubility. Environ. Geochem. Health 43 (7), 2757–2780. https://doi.org/10.1007/s10653-020-00770-5.

Misaki, K., Matsui, S., Matsuda, T., 2007. Metabolic enzyme induction by HepG2 cells exposed to oxygenated and nonoxygenated polycyclic aromatic hydrocarbons. Chem. Res. Toxicol. 20, 2736–2743.

Nahta, R., Al-Mulla, F., Al-Temaimi, R., et al., 2015. Mechanisms of environmental chemicals that enable the cancer hallmark of evasion of growth suppression. Carcinogenesis 36 (Suppl. 1), S2–18. https://doi.org/10.1093/carcin/bgv028.

Nemmar, A., Holme, J.A., Rosas, I., Schwarze, P.E., Alfaro-Moreno, E., 2013. Recent advances in particulate matter and nanoparticle toxicology: a review of the in vivo and in vitro studies. Biomed. Res. Int. 2013, 279371 https://doi.org/10.1155/2013/279371.

Nesnow, S., Ross, J.A., Nelson, G., et al., 1994. Cyclopenta[cd]pyrene-induced tumorigenicity, Ki-ras codon 12 mutations and DNA adducts in strain a/J mouse lung. Carcinogenesis 15 (4), 601–606. https://doi.org/10.1093/carcin/15.4.601.

Novotna, A., Pavek, P., Dvorak, Z., 2011. Novel stably transfected gene reporter human hepatoma cell line for assessment of aryl hydrocarbon receptor transcriptional activity: construction and characterization. Environ. Sci. Technol. 45 (23), 10133–10139. https://doi.org/10.1021/es2029334.

O'Driscoll, C.A., Gallo, M.E., Hoffmann, E.J., et al., 2018. Polycyclic aromatic hydrocarbons (PAHs) present in ambient urban dust drive proinflammatory T cell and dendritic cell responses via the aryl hydrocarbon receptor (AHR) in vitro. PLoS One 13 (12), e0209690. https://doi.org/10.1371/journal.pone.0209690.

Øvrevik, J., Låg, M., Lecureur, V., et al., 2014. AhR and Arnt differentially regulate NF-κB signaling and chemokine responses in human bronchial epithelial cells. Cell Commun. Signal. 12, 48. https://doi.org/10.1186/s12964-014-0048-8.

Øvrevik, J., Refsnes, M., Låg, M., Holme, J.A., Schwarze, P.E., 2015. Activation of proinflammatory responses in cells of the airway mucosa by particulate matter: oxidant- and non-oxidant-mediated triggering mechanisms. Biomolecules 5 (3), 1399–1440. https://doi.org/10.3390/biom5031399.

Øvrevik, J., Refsnes, M., Låg, M., Brinchmann, B.C., Schwarze, P.E., Holme, J.A., 2017. Triggering mechanisms and inflammatory effects of combustion exhaust particles with implication for carcinogenesis. Basic Clin. Pharmacol. Toxicol. 121 (Suppl. 3), 55–62. https://doi.org/10.1111/bcpt.12746.

Pálková, L., Vondráček, J., Trilecová, L., et al., 2015. The aryl hydrocarbon receptor-mediated and genotoxic effects of fractionated extract of standard reference diesel exhaust particle material in pulmonary, liver and prostate cells. Toxicol. in Vitro 29 (3), 438–448. https://doi.org/10.1016/j.tiv.2014.12.002.

Pehnec, G., Jakovljević, I., 2018. Carcinogenic potency of airborne polycyclic aromatic hydrocarbons in relation to the particle fraction size. Int. J. Environ. Res. Public Health 15 (11). https://doi.org/10.3390/ijerph15112485.

Pyo, J.S., Kim, N.Y., Kang, D.W., 2022. Impacts of outdoor particulate matter exposure on the incidence of lung cancer and mortality. Medicina (Kaunas) 58 (9). https://doi.org/10.3390/medicina58091159.

Quintana, F.J., Basso, A.S., Iglesias, A.H., et al., 2008. Control of T(reg) and T(H)17 cell differentiation by the aryl hydrocarbon receptor. Nature 453 (7191), 65–71. https://doi.org/10.1038/nature06880.

Ryter, S.W., Alam, J., Choi, A.M., 2006. Heme oxygenase-1/carbon monoxide: from basic science to therapeutic applications. Physiol. Rev. 86 (2), 583–650. https://doi.org/10.1152/physrev.00011.2005.

Schiavo, B., Meza-Figueroa, D., Vizuete-Jaramillo, E., et al., 2022. Oxidative potential of metal-polluted urban dust as a potential environmental stressor for chronic diseases. Environ. Geochem. Health. https://doi.org/10.1007/s10653-022-01403-9.

Seinfeld, J., Pandis, S., 1998. Atmospheric Chemistry and Physics: From Air Pollution to Climate Change. Wiley-Interscience, NewYork.

Shao, J., Wheeler, A.J., Chen, L., et al., 2018. The pro-inflammatory effects of particulate matter on epithelial cells are associated with elemental composition. Chemosphere 202, 530–537. https://doi.org/10.1016/j.chemosphere.2018.03.052.

Skuland, T., Grytting, V.S., Låg, M., et al., 2022. Road tunnel-derived coarse, fine and ultrafine particulate matter: physical and chemical characterization and pro-inflammatory responses in human bronchial epithelial cells. Part Fibre Toxicol. 19 (1), 45. https://doi.org/10.1186/s12989-022-00488-5.

Srogi, K., 2007. Monitoring of environmental exposure to polycyclic aromatic hydrocarbons: a review. Environ. Chem. Lett. 5 (4), 169–195. https://doi.org/10.1007/s10311-007-0095-0.

Stafoggia, M., Oftedal, B., Chen, J., et al., 2022. Long-term exposure to low ambient air pollution concentrations and mortality among 28 million people: results from seven large European cohorts within the ELAPSE project. Lancet Planet Health 6 (1), e9–e18. https://doi.org/10.1016/s2542-5196(21)00277-1.

Świetlik, R., Trojanowska, M., 2022. Chemical fractionation in environmental studies of potentially toxic particulate-bound elements in urban air: a critical review. Toxics 10 (3). https://doi.org/10.3390/toxics10030124.

Tong, H.Y., Karasek, F.W., 1984. Quantitation of polycyclic aromatic hydrocarbons in diesel exhaust particulate matter by high-performance liquid chromatography fractionation and high-resolution gas chromatography. Anal. Chem. 56 (12), 2129–2134. https://doi.org/10.1021/ac00276a034.

Topinka, J., Rossner Jr., P., Milcova, A., et al., 2015. Day-to-day variability of toxic events induced by organic compounds bound to size segregated atmospheric aerosol. Environ. Pollut. 202, 135–145. https://doi.org/10.1016/j.envpol.2015.03.024.

USEPA, 2005. Guidelines For Carcinogen Risk Assessment. EPA/630/P-03?001F. US Environmental Protection Agency Risk Assessment Forum, Washington, DC.

USEPA, 2010. Development of a Relative Potency Factor (RPF) Approach for Polycyclic Aromatic Hydrocarbon (PAH) Mixtures: in Support of Summary Information on the Integrated Risk Information System (IRIS). Environmental Protection Agency; EPA/635/ R-08/012A, United States Washington (DC).

Velali, E., Papachristou, E., Pantazaki, A., et al., 2016. Cytotoxicity and genotoxicity induced in vitro by solvent-extractable organic matter of size-segregated urban particulate matter. Environ. Pollut. 218, 1350–1362. https://doi.org/10.1016/j.envpol.2016.09.001.

Vondráček, J., Machala, M., 2021. The role of metabolism in toxicity of polycyclic aromatic hydrocarbons and their non-genotoxic modes of action. Curr. Drug Metab. 22 (8), 584–595. https://doi.org/10.2174/1389200221999201125205725.

Vondrácek, J., Machala, M., Minksová, K., et al., 2001. Monitoring river sediments contaminated predominantly with polyaromatic hydrocarbons by chemical and in vitro bioassay techniques. Environ. Toxicol. Chem. 20 (7), 1499–1506.

Vondrácek, J., Umannová, L., Machala, M., 2011. Interactions of the aryl hydrocarbon receptor with inflammatory mediators: beyond CYP1A regulation. Curr. Drug Metab. 12 (2), 89–103. https://doi.org/10.2174/138920011795016827.

Vondráček, J., Pěnčíková, K., Neča, J., et al., 2017. Assessment of the aryl hydrocarbon receptor-mediated activities of polycyclic aromatic hydrocarbons in a human cell-based reporter gene assay. Environ. Pollut. 220 (Pt A), 307–316. https://doi.org/10.1016/j.envpol.2016.09.064.

Westerholm, R.N., Almen, J., Li, H., Rannug, J.U., Egebaeck, K.E., Graegg, K., 1991. Chemical and biological characterization of particulate-, semivolatile-, and gas-phase-associated compounds in diluted heavy-duty diesel exhausts: a comparison of three different semivolatile-phase samplers. Environ. Sci. Technol. 25 (2), 332–338. https://doi.org/10.1021/es00014a018.

WHO, 2000. Air quality guidelines for Europe. WHO Reg. Publ. Eur. Ser. V-x (91), 1–273.

Wincent, E., Le Bihanic, F., Dreij, K., 2016. Induction and inhibition of human cytochrome P4501 by oxygenated polycyclic aromatic hydrocarbons. Toxicol. Res. (Camb.) 5 (3), 788–799. https://doi.org/10.1039/c6tx00004e.

Wingfors, H., Sjodin, A., Haglund, P., Brorstrom-Lunden, E., 2001. Characterisation and determination of profiles of polycyclic aromatic hydrocarbons in a traffic tunnel in Gothenburg, Sweden. Atmos. Environ. 35, 6361–6369.

Zhou, X., Hu, R., Fang, Y., 2021. Source and spatial distribution of airborne heavy metal deposition studied using mosses as biomonitors in Yancheng, China. Environ. Sci. Pollut. Res. Int. 28 (24), 30758–30773. https://doi.org/10.1007/s11356-021-12814-z.

Ziou, M., Tham, R., Wheeler, A.J., Zosky, G.R., Stephens, N., Johnston, F.H., 2022. Outdoor particulate matter exposure and upper respiratory tract infections in children and adolescents: a systematic review and meta-analysis. Environ. Res. 210, 112969 https://doi.org/10.1016/j.envres.2022.112969.